Contemporary Mathematics
http://ojs.wiserpub.com/index.php/CM/

Research Article

Mathematical Modeling of Middle East Respiratory Syndrome Coronavirus with Bifurcation Analysis

Mehmet Yavuz[1*], Mati ur Rahman[2,3], Mustafa Yildiz[4], Hardik Joshi[5]

[1] Department of Mathematics and Computer Sciences, Faculty of Science, Necmettin Erbakan University, Konya 42090, Turkey
[2] School of Mathematical Sciences, Jiangsu University, Zhenjiang 212013, Jiangsu P.R. China
[3] Department of Computer Science and Mathematics, Lebanese American University, Beirut, Lebanon
[4] Department of Mathematics, Bartın University, Bartın 74100, Turkey
[5] Department of Mathematics, LJ Institute of Engineering and Technology, LJ University, Ahmedabad, Gujarat, 382210 India
E-mail: mehmetyavuz@erbakan.edu.tr

Received: 22 May 2024; **Revised:** 20 August 2024; **Accepted:** 21 August 2024

Abstract: The Middle East respiratory syndrome is a viral respiratory illness. It is caused by a common type of virus called coronavirus. The main objective of the present work, we develop a mathematical model for the transmission dynamics of the Middle East respiratory syndrome coronavirus (MERS-CoV) disease. To assess the transmissibility of the MERS-CoV, we calculate the basic reproduction number $\mathfrak{R}_0$. Furthermore, the existence of the backward bifurcation for different parameters is presented. The sensitivity analysis is presented to analyze the importance of various epidemic parameters. Stability analysis for the model is examined to provide stability conditions. Finally, we present the numerical simulations of the proposed model to support our analytical findings.

***Keywords*:** basic reproduction number, backward bifurcations, sensitivity analysis, stability, numerical simulation

MSC: 65L05, 34K06, 34K28

1. Introduction

Middle Eastern respiratory syndrome coronavirus is a new type of coronavirus, it was first reported in the Kingdom of Saudi Arabia (KSA) in 2012 [1, 2]. MERS is mostly connected with animal sources. MERS-CoV has also been found in camels in different countries. Humans may become infected after coming into touch with camels. Coughing transfers illness from one to another. MERS-CoV is transmitted from infected individuals to others through intimate contact, such as looking after or living with the infected individuals. There has been a total number of 536 cases which includes 145 deaths since April 2012, a rate of death 27%, with the bulk of cases recorded in the Middle East (KSA, Qatar and Jordan) [3]. MERS-CoV-infected persons experienced a severe abrupt respiratory infection with symptoms including cough, fever, and breathlessness.

The virus is mostly spread by dromedary camels, according to scientific evidence. Most human infections (75%) are caused by human-human transmissions, with the remaining instances caused by camel-human transmissions.

Mathematical modeling is vital for studying and forecasting the evolution of infectious illnesses [4]. Assire et al. [5] documented one of the biggest MERS-CoV epidemics, with the characterization that the viral disease is transmittable from

DOI: https://doi.org/10.37256/cm.5320245004

person to person. In a review paper, Zumla et al. [6] highlighted that even the cause for camel-human transmission might be exposed indirectly, e.g., the patient's exposure to MERS-CoV could have been through intake of raw or unprocessed camel milk, which is a widespread practice in KSA.

The derivative and integration of non-integer and real-order functions can be defined and developed with the aid of fractional calculus. Fractional derivatives are a convenient and precise way to describe many scientific phenomena that cannot be understood using integer order derivatives. Fractional order differential equations illustrate the idea of system memory. Numerous fractional derivatives, including Caputo, Hadamard, Grünwald-Letnikov, Riesz, and Riemann-Liouville fractional derivatives, are available in the literature [7–9]. There are numerous analytical techniques that cannot handle a wide variety of equations and are severely restricted in their application found in the literature. Numerical techniques and approaches are created to determine the solution of fractional differential equations due to the difficulty of applying analytical methods. Several works have been published in the literature on mathematical modelling by applying the approach of fractional, fractal-fractional differential equations and fuzzy differential equations [10–17], HCV model [18], finance model [19, 20] and several other analytical and numerical scheme have been investigated such as [21–25].

Mathematical modeling is very important for the transmission dynamics of different diseases for mathematicians and researchers. Numerous works have been documented for the different types of research related to disease, economics, engineering and other many applicable areas [26–29]. Researchers investigated various aspects and defined the application of modeling in real life by applying the approach of fractional calculus and mentioned their behavior and the impact on society [30–33].

In this study, we construct a five-compartmental MERS-CoV model for the transmission dynamics of disease including susceptible population $S(t)$, exposed population $E(t)$, symptomatic (infected) population $I(t)$, recovered population $R(t)$, and reservoir population $C(t)$ for MERS-CoV. The proposed model stability is investigated respectively. The basic reproductive number $\mathfrak{R}_0$ is calculated for the model to determine the stability condition. By using the next-generation matrix approach, we develop a formula for $\mathfrak{R}_0$ of the camels-human population to determine transmissibility potential. A sensitivity study is done for the parameters in the model in order to obtain their impact on the transmission of the suggested disease. Backward bifurcation is very important in a disease model. Therefore the backward bifurcation and also the endemic equilibria are analyzed for the proposed model accordingly.

To study the stability of the proposed model (1), we utilize the Routh-Hurwitz (R-H) criteria. In case $\mathfrak{R}_0 < 1$ the disease-free equilibrium (DFE) of the proposed problem, then the model is locally asymptotically stable (LAS) therefore there is no disease after the passage of time. While $\mathfrak{R}_0 > 1$, the disease remains in the population. Also, we analyze the model for global stability with the aid of the theory of Lyapunov function. Graphical simulations of the system (1) are displayed.

The structure of this paper is as follows: we represent the formulation of the considered problem in Section 2. Section 3 shows the well-posedness of the model and basic reproductive number. Section 4 deals with backward bifurcations, sensitivity analysis and EE. In Section 5, we discuss local and global stability analysis of the equilibria. In Section 6, numerical simulations and graphical illustrations are presented. Finally, in Section 7, we give the concluding remarks for the work.

2. Model formulation

The section shows the mathematical construction of the deterministic model for MERS-CoV transmission. This model is composed of differential equations (DEs). We develop the model by taking into account the characteristics of the disease.

a. All parameters and the variables are non-negative.

b. Two transmission routes are considered for the disease transmission, which are from symptomatic individuals and then reservoir, which are camels for MERS-CoV.

c. The rate of death because of MERS-CoV is considered in the compartment that contains the infection.

The dynamics in the host population are,

$$\frac{dS}{dt} = \pi - \beta S(t)E(t) - \psi\beta S(t)I(t) - (\delta\beta C(t) + \mu_0)S(t),$$

$$\frac{dE}{dt} = \beta S(t)E(t) + \psi\beta S(t)I(t) + \delta\beta C(t)S(t) - (\alpha + \mu_0)E(t),$$

$$\frac{dI}{dt} = \alpha E(t) - (\eta_2 + \eta_1)I(t) - (\mu_0 + \mu_1)I(t),$$

$$\frac{dR}{dt} = (\eta_2 + \eta_1)I(t) - \mu_0 R(t),$$

$$\frac{dC}{dt} = \varpi_1 E(t) + \varpi_2 I(t) - dC(t), \tag{1}$$

depends on conditions

$$S(0) > 0, E(0) \geq 0, I(0) \geq 0, R(0) \geq 0, C(0) \geq 0. \tag{2}$$

In model (1) the description of the parameters is given below and we mentioned the flowchart in Figure 1:

- π represents susceptible recruitment rate;
- μ_0 is natural death rate and μ_1 is the death rate by disease;
- β is the rate of transmission;
- ψ denotes rate of approximate transmission of infectious people. The rate at which the population from the exposed class goes to the infected class by α;
- ϖ_1 is the rate at which the exposed individuals are in contact with the reservoir;
- d is the life time of reservoir;
- η_1, η_2 is the rate at which the infected individual become recover;
- ϖ_2 is the rate at which the infected individual are in contact with reservoir;

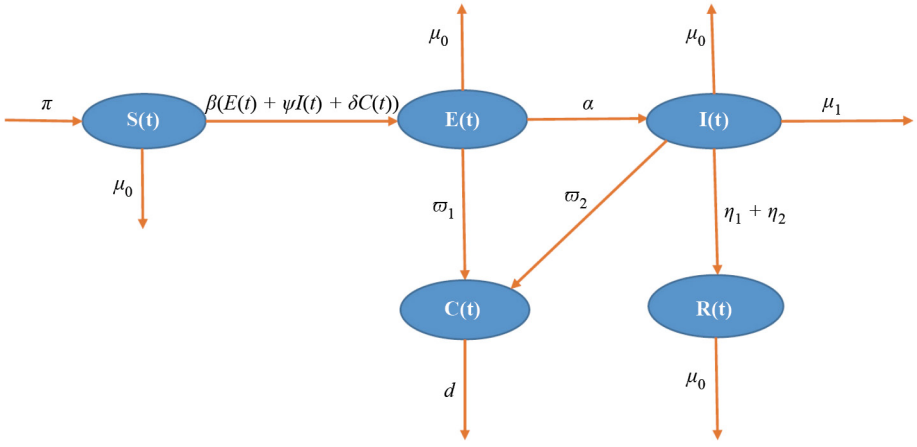

Figure 1. Diagram of MERS-Cov disease transmission

3. Well-posedness of the problem

Suppose $\mathfrak{P}(t)$ stands for total population of humans i,e $\mathfrak{P}(t) = S(t)+I(t)+R(t)+E(t)$, so the population has bounds, lower & upper bounds to be 0 and $\frac{\pi}{\mu_0}$, respectively, such that, $0 \leq \mathfrak{P}(t) \leq \frac{\pi}{\mu_0}$.

Using this fact as a basis we provide the theorem below.

Theorem 1 If $\mathfrak{P}(t)$ is total human population, also $0 \leq \mathfrak{P}(t) \leq \frac{\pi}{\mu_0}$, and $\mathfrak{P}(t) \leq \frac{\pi}{\mu_0}$, so the problem (1) lies in the region given below.

$$\Omega = \left\{ (S, E, I, R, C) \in R_+^5, \mathfrak{P}(t) \leq \frac{\pi}{\mu_0}, C \leq \frac{(\varpi_1 + \varpi_2)\pi}{\mu_0} \right\}.$$

Proof. Let us consider B_s is a Banach space, and e_+ which is positive, so

$$B_s = q^1(0, e_+) \times q^1(0, \rho_+) \times q^1(0, \rho_+) \times q^1(0, \rho_+) \times q^1(0, \rho_+). \tag{3}$$

Norm on B_{s+} is $\|\xi\| = \sum_{i=1}^5 \|\xi_j\|$, here $\|\xi\| = (\xi_1, \xi_2, \xi_3, \xi_4, \xi_5) \in B_{s+}$.
Further, B_{s+} is the cone (positive) of $q^1(0, e_+)$, so from Eq. (3), B_{s+} becomes

$$B_s = q^1(0, e_+) \times q^1(0, \rho_+) \times q^1(0, \rho_+) \times q^1(0, \rho_+) \times q^1(0, \rho_+).$$

Hence the state space of system (1) yields:

$$\Lambda = \left\{ (S, E, I, R, C \in B_{s+} \ni 0 \leq \mathfrak{P}(t) \leq \frac{\pi}{\mu_0} \right.$$

$$\left. 0 < S(t) + R(t) + I(t) + A(t) \leq \frac{\pi}{\mu_0}, C \leq \frac{(\varpi_1 + \varpi_2)\pi}{\mu_0} \right\}.$$

□

We consider an operator which is linear denoted by D and also consider vector $\Psi = (S, E, I, R, C)$, implying $D\Psi = (D_1, D_2, D_3, D_4, D_5)^T$, where

$$\begin{aligned}
D_1 &= (-\frac{dS}{dt} - \mu_0 S, 0, 0, 0, 0), \\
D_2 &= (0, -\frac{dE}{dt} - (\alpha + \mu_0)E, 0, 0, 0), \\
D_3 &= (0, \alpha E, -\frac{dI}{dt} - (\eta_1 + \eta_2 + \mu_0 + \mu_1), 0, 0), \\
D_4 &= (0, 0, (\eta_1 + \eta_2)I, -\frac{dR}{dt} - \mu_0 R, 0),
\end{aligned}$$

$$D_5 \quad = \quad (0, 0, \varpi_1 E, \varpi_2 I, 0, 0, -\frac{dC}{dt} - dC),$$

and domain of D, D(L) is

$D(L) = \left\{ \varpi \in B_s \colon \Psi \in LC[0, e_+), \varpi(0) = (S_0, E_0, I_0, R_0, C_0) \right\}$. Here, $LC[0, e_+)$ is the set having functions which are continuous defined on interval $[0, e_+)$. Consider M is the operator which is nonlinear i.e. $M \colon B_s \to B_s$ by,

$$M(\psi) = \begin{pmatrix} \pi - \beta ES - \beta \psi IS - \delta \beta CS \\ \beta ES + \beta \psi IS + \beta \delta CS \\ 0 \\ 0 \\ 0 \end{pmatrix}. \tag{4}$$

Suppose $z(t) = (S(t), E(t), I(t), R(t), C(t))$ then the suggested system is

$$\frac{dz}{dt} = L(z(t)) + M(z(t)), z(0) \in B,$$

where $z(0) = (S_0, E_0, I_0, R_0, C_0)^T$. With the use of result [34, 35], we present existence of the solution of model (4), so we immediately state results as follows:

Theorem 2 For each $v(0) \in B_{s+}$, there exist maximal interval and unique continuous solution $[0, t_0)$ and $v(t, v_0)$ respectively, such that,

$$v(t) = v_0 e^{Lt} + \int e^{L(t-r)} M(v(\tau)).$$

Theorem 3 The model (1) is invariant (positively) subjected to nonnegative orthant R^5+.

Proof. As we have $\varpi = (S, E, I, R, C)$. Let $r_1 = (\alpha + \mu_0)$, $r_2 = (\eta_1 + \eta_2 + \mu_1 + \mu_0)$, $r_4 = (\varpi_1 + \varpi_2 + d)$,

$$\frac{d\varpi}{dt} = L\varpi + D$$

$$L = \begin{bmatrix} -\mu_0 & 0 & 0 & 0 & 0 \\ 0 & -r_1 & 0 & 0 & 0 \\ 0 & \alpha & -r_2 & 0 & 0 \\ 0 & 0 & \eta_1 & \eta_2 & 0 \\ 0 & 0 & \varpi_1 & \varpi_2 & -d \end{bmatrix}, T = \begin{bmatrix} \pi \\ 0 \\ 0 \\ 0 \\ 0 \end{bmatrix}. \tag{5}$$

It could be noted from Eq. (5), that T matrix is positive, while the off-diagonal of the L are non-negative, therefore the properties of the Metzler matrix are satisfied. So the model under study is invariant in R^5. □

Theorem 4 We consider the size of the population initially for the suggested system presented in (2) if solutions Eq. (1) exist, it will remain positive for all e_+.

Proof. Let us consider the susceptible population

$$\frac{dS}{dt} = \pi - \beta ES - \beta \psi IS - (\beta CS + \mu_0)S. \tag{6}$$

Utilizing the alternation of the constants formula, we obtain the solution to Eq.(6),

$$\begin{aligned} S &= S_{(0)} \exp\left[-dt - \int [\beta E - \beta \psi I - \beta \delta C] S\right] dx \\ &\quad + \Pi \exp\left[-dt - \int [\beta E - \beta \psi I - \beta \delta C] S\right] dx \\ &\quad \times \left[dt + \int [\beta E + \beta \psi I + \beta \delta C] S\right] dx. \end{aligned}$$

$S > 0$, likewise one can show that, the remaining equations of model (1) are also positive. □

3.1 *Possible equilibria and basic reproduction number*

There exist two different equilibria: the first one is DFE and the second one is endemic equilibrium (EE). The DFE of system (1) is denoted with F_0 and defined for the $F_0 = (S_0, 0, 0, 0, 0)$, and

$$S_0 = \frac{\pi}{\mu_0}. \tag{7}$$

$\Re_0$ is defined as the quantity that determines whether an epidemic will occur or if the disease will die off. Which is the estimated average number of infections due to a single infectious agent, both directly and indirectly, in a completely susceptible population. Driessche approach is used to calculate the reproduction number [36]. Suppose

$$\frac{d\chi}{dt} = \bar{F} - \bar{V}. \tag{8}$$

In equation (8), here $\bar{F}$ and $\bar{V}$ are matrices having nonlinear, and linear terms respectively, that is

$$\bar{F} = \begin{pmatrix} (\beta E(t) + \psi \beta I(t) + \delta \beta C(t))S(t) \\ 0 \\ 0 \end{pmatrix},$$

$$\bar{V} = \begin{pmatrix} -(\alpha+\mu_0)E(t) \\ \alpha E(t) - (\eta_1+\eta_2+\mu_0+\mu_1)I(t) \\ \varpi_1 E(t) + \varpi_2 I(t) - dC(t) \end{pmatrix}.$$

The Jacobian of $\bar{F}$ and $\bar{V}$ at DFE F_0, that is

$$F = \text{Jacobian of } \bar{F} \text{at } DFE = \begin{pmatrix} \beta S_0 & \psi\beta S_0 & \delta\beta S_0 \\ 0 & 0 & 0 \\ 0 & 0 & 0 \end{pmatrix},$$

$$V = \text{Jacobian of } \bar{V} \text{at } DFE = \begin{pmatrix} (\alpha+\mu_0) & 0 & 0 \\ -\alpha & (\eta_1+\eta_2+\mu_0+\mu_1) & 0 \\ -\varpi_1 & -\varpi_2 & d \end{pmatrix}.$$

Therefore $\mathfrak{R}_0$ stands for the spectral radius of matrix $\bar{H} = FV^{-1}$ which is next-generation matrix, hence $\mathfrak{R}_0$ for model (1) is

$$\mathfrak{R}_0 = \frac{\beta\pi}{\mu_0(\alpha+\mu_0)} + \frac{\beta\alpha\psi\pi}{\mu_0(\alpha+\mu_0)(\eta_1+\eta_2+\mu_0+\mu_1)} + \frac{\beta\delta\pi(\alpha\varpi_2+\eta_1\varpi_1+\eta_2\varpi_1+\varpi_1\mu_0+\varpi_1\mu_1)}{d(\alpha+\mu_0)(\eta_1+\eta_2+\mu_0+\mu_1)}. \tag{9}$$

The $\mathfrak{R}_0$ is made up of two elements that reflect two separate transmission channels from infected persons to susceptible people: from the environmental reservoir to the susceptible population. These two mechanisms of transmission combine to determine the epidemic's overall illness risk.

4. Endemic equilibria and bifurcation analysis

We suppose that the LHS of the differential equation (1) is 0, then endemic (S, E, I, R, C) fulfils $S > 0$, $E > 0$, $I > 0$, $R >$, $C > 0$ and

$$S^* = \frac{(\alpha+\mu_0)(\eta_1+\eta_2+\mu_0+\mu_1)}{\beta(\eta_1+\eta_2+\mu_0+\mu_1)+d\mu\mu_0\beta+\delta\beta\varpi_1(\eta_1+\eta_2+\mu_0+\mu_1)+\varpi_2\mu_1\delta\beta},$$

$$E^* = \frac{d\mu_0(\alpha+\mu_0)(\beta(\eta_1+\eta_2+\mu_0+\mu_1))}{(\mu_0+\alpha)(\beta(\eta_1+\eta_2+\mu_1+\mu_0)+d\mu_0\mu_1\beta+\delta\beta\varpi_1(\eta_1+\eta_2+\mu_0+\mu_1)+\varpi+2\varpi_1\delta\beta)},$$

$$R^* = \frac{\mu_1(\eta_1+\eta_2+\mu_0+\mu_1)+\mu_1 d\varpi_2}{\mu_0(\eta_1+\eta_2+\mu_0+\mu_1)}.$$

Putting the value of expression presented above into the very first sub-equation of model (1) and after a little bit of work, we obtain

$$b_1 I^2 + b_2 I + b_3. \tag{10}$$

$$b_1 = \frac{\beta\mu_0(\mu_0+\alpha)+(\mu_0+\alpha)(\Re_0-1)}{(\mu_0+\mu_1+\eta_1+\eta_2)} + \frac{\beta d(\mu_0+\alpha)}{(\mu_0+\mu_1+\eta_1+\eta_2}),$$

$$b_2 = -\mu_1\beta - \beta(\mu_0+\alpha) - \frac{\mu_0\mu_1\delta\beta}{(\mu_0+\alpha)} - (1-\Re_0),$$

$$b_3 = \mu_0(\mu_0+\alpha)(\Re_0-1).$$

If $\Re_0 > 1$, then $b_3 > 0$, $b_1 > 0$, it shows that system (1) gets unique EE $E^* = (S^*, E^*, I^*, R^*)$. If $\Re_0 < 1$, we have $b_1 < 0$, $b_2 < 0$, $b_3 < 0$ which has no EE.

The importance of the backward bifurcations for epidemiological models is similar to that same classical need for $\Re_0$ to be smaller than one [37, 38], which is required for the MERS-CoV virus to be eradicated from the community. Backward bifurcation complicates disease control strategies. Backward bifurcating diseases can continue to exist in a population even when their rate of reproduction indicates they should go extinct. The existence of the backward bifurcations in the suggested model shows that when $\Re_0$ is less than one, the feasibility of MERS-CoV removal is dependent on the starting size of the model's sub-population. when $\Re_0 = 1$, then the following are satisfied.

Lemma 1 If $\Re_0 = 1$, then system (1) has backward bifurcation phenomena when $b_3 < 0$ (see Figure 2).

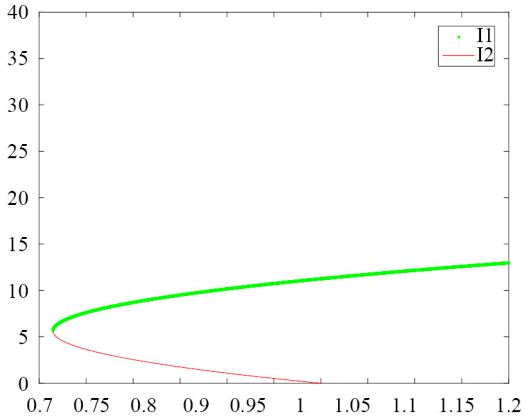

Figure 2. Backward Bifurcation in model (1)

4.1 *Sensitivity analysis*

The suggested model's parameters are subjected to sensitivity analysis. This approach will make it easy to identify the variables that have a significant impact on $\mathfrak{R}_0$. We utilize the technique presented in [39] and given as, $\Delta_h^{\mathfrak{R}_0} = \frac{\partial \mathfrak{R}_0}{\partial h} \frac{h}{\mathfrak{R}_0}$ here h is a parameter.

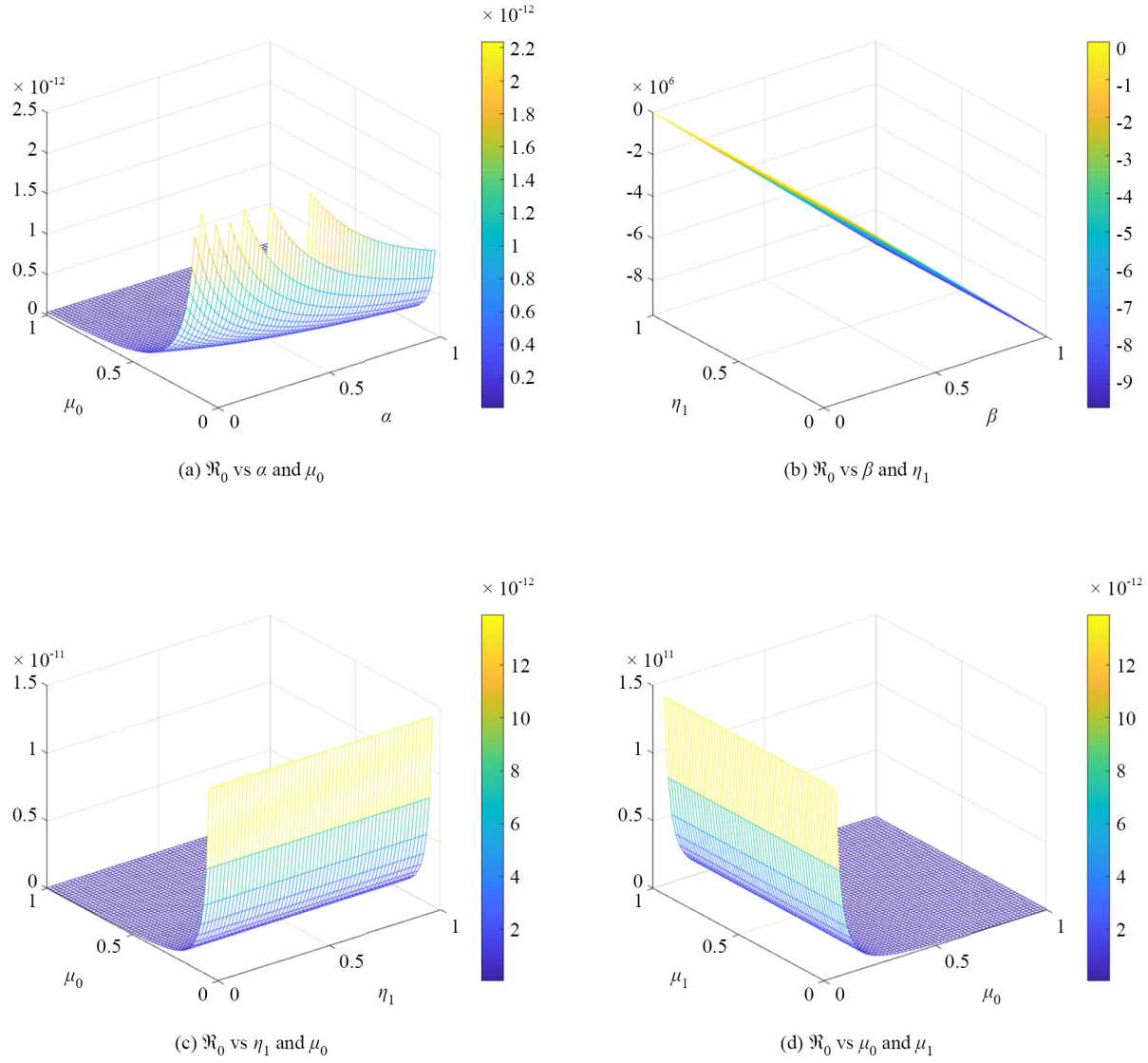

(a) $\mathfrak{R}_0$ vs α and μ_0

(b) $\mathfrak{R}_0$ vs β and η_1

(c) $\mathfrak{R}_0$ vs η_1 and μ_0

(d) $\mathfrak{R}_0$ vs μ_0 and μ_1

Figure 3. The effects of different parameters on the $\mathfrak{R}_0$ and variations in them

Figure 3 and Figure 4 depict the sensitivity analysis of $\mathfrak{R}_0$. They depict the significance of various parameters during disease transmission. It also measures the variation in $\mathfrak{R}_0$ with respect to the changes in the parameters.

It is obvious from the sensitivity that there exist direct relations between $\mathfrak{R}_0$ and the parameters set. $S_1 = [\beta, \delta, \eta_1, \eta_2, \pi, \psi, \varpi_1, \varpi_2]$, while has the inverse relation with $S_2 = [\mu_0, \delta]$. This shows that an increase in the values of the parameters set S_1 obviously increases threshold quantity, on the other hand increasing the values of parameters S_2 decreases threshold quantity. The model parameters and their sensitivity values according to $\mathfrak{R}_0$ are given in Table 1.

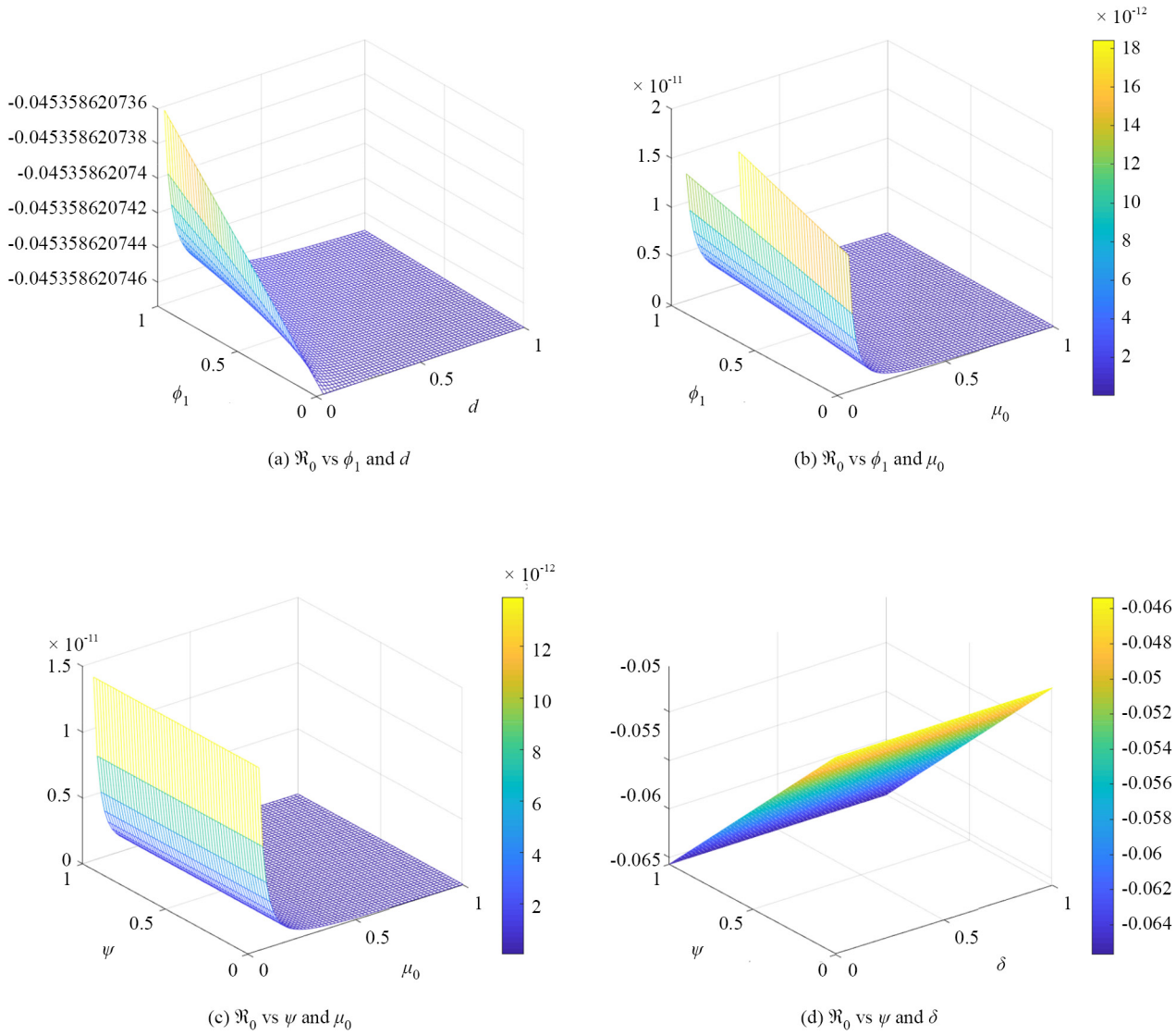

(a) $\Re_0$ vs ϕ_1 and d

(b) $\Re_0$ vs ϕ_1 and μ_0

(c) $\Re_0$ vs ψ and μ_0

(d) $\Re_0$ vs ψ and δ

Figure 4. The effects of different parameters on the $\Re_0$ and variations in them

Table 1. Parameter values and their sensitivity values

Parameter	Sensitivity values	Parameter	Sensitivity values
β	0.00000947	α	0.00047015
η_1	0.00013789	π	0.00009370
δ	-0.00093984	μ_0	-0.0084532
ϖ_1	0.0004498	ϖ_2	0.00094896
η_2	0.0000515	ψ	0.000043
μ_1	0.00068945	d	0.0000102

5. Stability analysis

Here, we present the local asymptotic stability of the DFE as well as the EE of the problem (1) in the theorems presented below.

Theorem 5 The DFE point $(F_0, 0, 0, 0)$ is stable locally asymptotically when $\Re_0 < 1$ otherwise not.

Proof. To show the local stability of the aforementioned model, for the points $(F_0, 0, 0, 0)$, let us consider the Jacobian of system (1)

$$J_0 = \begin{pmatrix} -\mu_0 & -\frac{\beta\pi}{\mu_0} & -\frac{\psi\beta\pi}{\mu_0} & -\frac{\delta\beta\pi}{\mu_0} \\ 0 & \frac{\beta\pi}{\mu_0} - (\mu_0+\alpha) & \frac{\psi\beta\pi}{\mu_0} & \frac{\delta\beta\pi}{\mu_0} \\ 0 & \alpha & -(\eta_1+\eta_2+\mu_0+\mu_1) & 0 \\ 0 & \varpi_1 & \varpi_2 & -d \end{pmatrix}. \tag{11}$$

In the above matrix the eigenvalues of the first two have real-part, $-\mu_0 < 0$, $-(\mu_0+\alpha) < 0$ while for the other eigenvalues we consider a 2×2 matrix,

$$J_0 = \begin{pmatrix} \frac{\beta\pi}{\mu_0} - (\mu_0+\alpha) & \frac{\beta\psi\pi}{\mu_0} \\ \alpha & -(\eta_1+\eta_2+\mu_0+\mu_1) \end{pmatrix}. \tag{12}$$

Now for Routh-Hurwitz criteria [40], it is enough to show that, the trace of the matrix A is negative and its determinant is positive, if $\Re_0 < 1$, hence we get

$$\begin{aligned} Trace(A) &= [\frac{\beta\pi}{\mu_0} - (\mu_0+\alpha)] + [-(\eta_1+\eta_2+\mu_0+\mu_1)], \\ Trace(A) &= -[(\mu_0+\alpha) + (\eta_1+\eta_2+\mu_0+\mu_1) - \frac{\beta\pi}{\mu_0}]. \end{aligned}$$

Thus, the $Trace(A) < 0$ if $\Re_0 < 1$. Now for the determinant, we have

$$\begin{aligned} \det(A) &= [\frac{\beta\pi}{\mu_0} - (\mu_0+\alpha)][-(\eta_1+\eta_2+\mu_0+\mu_1)] - \frac{\beta\pi\delta}{\mu_0}, \\ \det(A) &= [-(\frac{\beta\pi}{\mu_0})(\eta_1+\eta_2+\mu_0+\mu_1) + ((\mu_0+\alpha)], \\ \det(A) &= (\mu_0+\alpha)(\eta_1+\eta_2+\mu_0+\mu_1)[1 - (\frac{\beta\pi}{\mu_0(\mu_0+\alpha)} + \frac{\mu_1\pi}{\mu_0(\mu_0+\alpha)(\eta_1+\eta_2+\mu_0+\mu_1)} \\ &\quad + \frac{\beta\delta\pi(d\eta_1+d\eta_1+\eta_2\alpha+\eta_1+\eta_2)}{d(\mu_0+\alpha)(\eta_1+\eta_2+\mu_0+\mu_1))}] + \beta\delta\pi(\mu_0\varpi_1+\mu_1\varpi_1+\varpi_2+\varpi_1\eta_2+\varpi_1\mu_1. \\ \det(A) &= (\mu_0+\alpha)(\eta_1+\eta_2+\mu_0+\mu_1)(1-\Re_0) + \beta\delta\pi(\mu_0\varpi_1+\mu_1\varpi_1+\varpi_2+\varpi_1\eta_1+\eta_2\varpi_2. \end{aligned}$$

Hence, $\det(A) > 0$ if $\Re_0 < 1$, which shows that $\det(A)$ is positive, when $\Re_0 < 1$. Hence, $Trac(A) < 0$ and $\det(A) > 0$ $\Leftrightarrow \Re_0 < 1$. So that the DFE is locally asymptotically stable at F_0. □

5.1 *Global stability analysis*

The theorems presented below provide the global stability at DFE point F_0. To analyze the global stability at F_0 we develop the following Lyapunov function.

Theorem 6 If $\Re_0 < 1$ the DFE of the system is globally asymptotically stable if $S = S^0$.

Proof. Let us set up the following Lyapunov function,

$$\tau(t) = [\Re_1(S - S^0) + \Re_2 E(t) + \Re_3 I(t) + \Re_4 C]. \tag{13}$$

Here $\Re_i$ for $i = 1, 2, 3, 4,$ are some arbitrary constants, they are considered later by the differentiation of Eq.(13) , and using (1), we obtain

$$\begin{aligned}
\tau'(t) &= \Re_1[\pi - (\beta E(t) + \psi\beta I(t) + \delta\beta C(t) + \mu_0)S(t)] + \Re_2[(\beta E(t) + \psi\beta I(t) \\
&\quad -(\mu_0 + \alpha)E(t)] + \Re_3[\alpha E(t) - (\eta_1 + \eta_2 + \mu_0 + \mu_1)I(t)] + \Re_4[\varpi_1 I(t) + \varpi_2 I(t) - dC(t)] \\
\frac{\pi}{\mu_0} &= S_0,\ \pi = \mu_0 S_0 \\
\tau'(t) &= -[\Re_1(\mu_0 S - \mu_0 S_0) + (\Re_1 - \Re_2)(\beta E(t) + \psi\beta I(t) + \delta\beta C(t) + \mu_0)S(t)) + \Re_4(\Re_2 - \Re_3)\alpha E(t) + \mu_0\Re_2 E(t) \\
&\quad +\Re_3\mu_1 I(t) + \mu_0\Re_3 I(t) + \Re_3(\eta_1 + \eta_2)I - \Re_4\varpi_1 E(t) - \Re_4\varpi_2 I(t)].
\end{aligned}$$

By choosing the positive parameter $\Re_1, \Re_2, \Re_3, \Re_4$

$$\begin{aligned}
\tau'(t) &= -[\beta[(\mu_0(S - S_0) + \alpha(\eta_1 + \eta_2 + \mu_0 + \mu_1)(1 - \Re_0) + (\mu_0\alpha - (\varpi_1 + \varpi_2 + \mu_0)\eta_1)E \\
&\quad +(2\mu_0\alpha + (\varpi_1 + \varpi_2 + \mu_0)(\eta_1 + \eta_2 + \mu_0 + \mu_1)\eta_2)I].
\end{aligned}$$

$\tau'(t)$ is negative if $S > S^0$ and also $\Re_0 < 1$ and $\tau'(t) = 0$ if $S = S^0$. By invariance principle [41], and $E = I = C = 0$. hence the DFE is globally asymptotically stable in F_0. □

6. Numerical simulations

In this section, we obtained the solution of the suggested model by using the RK4 technique [42]. This verifies our analytical calculations. For simulation, we consider various values of parameters present in the suggested model which are presented in Table 2. The values of the parameter are used in such a way that is far more biologically realistic. The initial value for the population $S(t)$, $I(t)$, $E(t)$, $R(t)$, and $C(t)$ is 10 weeks. The biological interpretation of these figures shows that for $\Re_0 < 1$, the susceptible population decreases and then becomes stable and shows that there will be always

a susceptible population. The interpretation of $E(t)$, $I(t)$, $R(t)$ and $C(t)$ show that these populations first decreases and reaches zero as shown in Figure 5 to Figure 6, while the dynamics of the camel population that is a reservoir for camel reveals that the camel population decreases up to 70 days while then reaches its equilibrium position, this ensures that there will be always camel population. These ensure the stability of the proposed model for the reproduction number less than 1. From the figures, we observe that the decline in the cures goes to the stable point. By emphasizing important intervention points like minimizing human-animal contact and enhancing treatment and isolation measures, this model assists in comprehending the dynamics of the disease and provides guidance for public health policies.

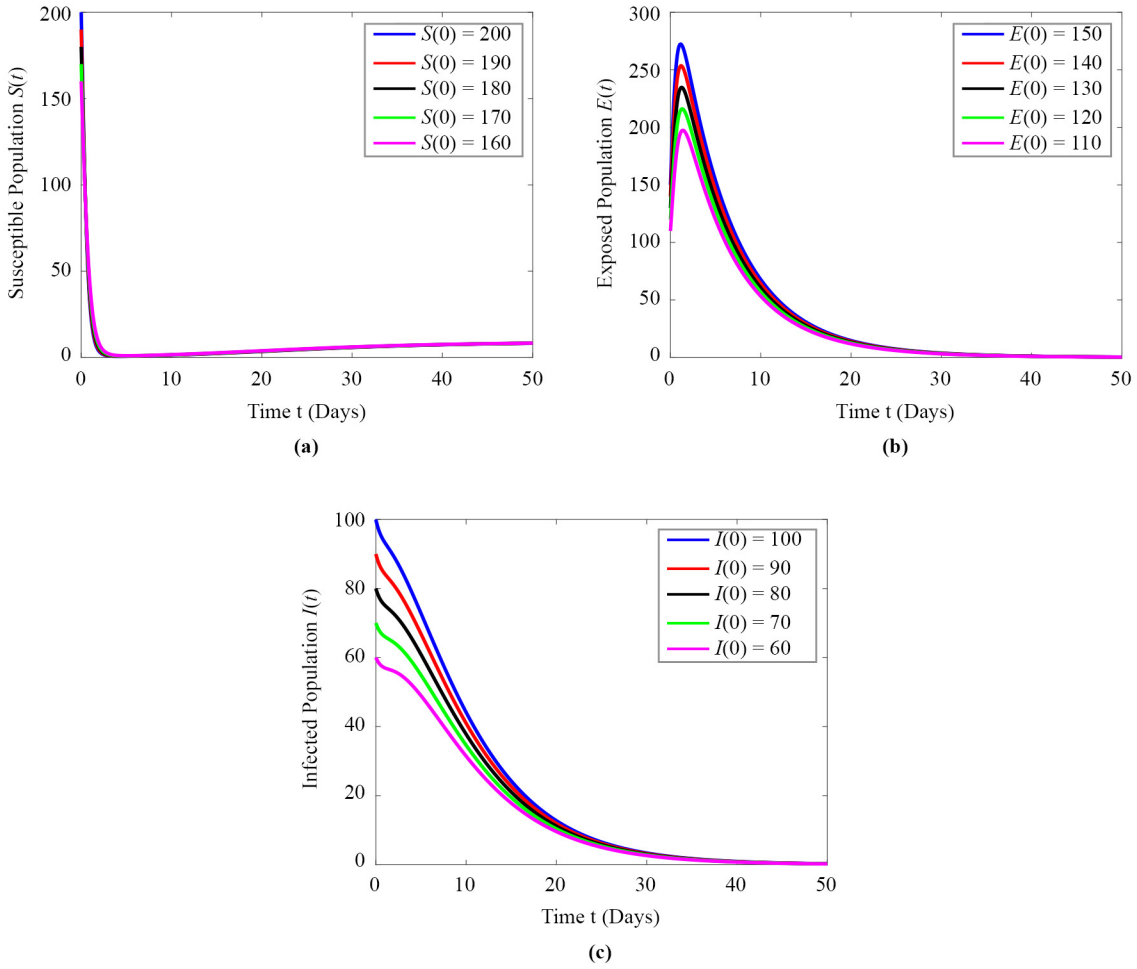

Figure 5. Dynamical behaviors for the classes $(a) = S(t)$, $(b) = E(t)$ and $(c) = I(t)$ of the considered model of different compartments

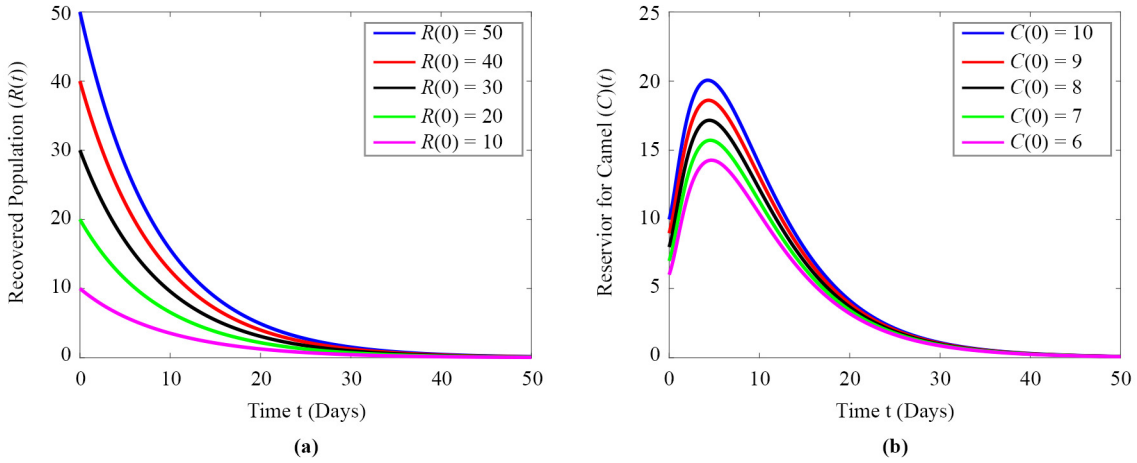

Figure 6. Dynamical behaviors for the classes $(a) = R(t)$ and $(b) = C(t)$ of the considered model of different compartments

Table 2. Parameters and their values

Parameters	Values	Sources	Parameters	Values	Sources
π	0.09	[39]	μ_0	0.022	assumed
ψ	0.26	assumed	δ	0.02	assumed
α	0.05	assumed	μ_1	0.065	assumed
η_1	0.02	assumed	η_2	0.04	assumed
ϖ_1	0.04	assumed	ϖ_2	0.014	assumed
d	0.01	assumed	β	0.08	[42]

7. Concluding remark

In this work, we have formulated a mathematical model to analyze the transmission dynamics of MERS-CoV. This work provides a platform to investigate some challenges in the area of research and realization of the qualitative behavior of MERS-CoV. The basic reproductive number $\mathfrak{R}_0$ is calculated for the suggested problem to study the transmission rate of MERS-CoV. We have discussed the existence of backward bifurcations for a range of parameters. For the significance of the epidemic parameters, the sensitivity analysis is studied. From the sensitivity analysis, we observe that an increase in the values of the parameters set S_1 obviously increases threshold quantity, on the other hand increasing the values of parameters S_2 decreases threshold quantity. We have discussed the local and global stability of the suggested model for $\mathfrak{R}_0 < 1$.

In the future, we can further extend the work by taking optimal control of the proposed model to minimize the MERS CoV-infected population. We can also extend this model to a fractional order differential equation to point out the memory trace and hereditary features.

Conflict of interest

The authors declare no competing financial interest.

References

[1] Azhar EI, El-Kafrawy SA, Farraj SA, Hassan AM, Al-Saeed MS, Hashem AM, et al. Evidence for camel-to-human transmission of Mers coronavirus. *New England Journal of Medicine*. 2014; 370(26): 2499-2505.

[2] Arabi YM, Arifi AA, Balkhy HH, Najm H, Aldawood AS, Ghabashi A, et al. Clinical course and outcomes of critically ill patients with Middle East respiratory syndrome coronavirus infection. *Annals of Internal Medicine*. 2014; 160(6): 389-397.

[3] Fisman DN, Tuite AR. The epidemiology of Mers-Cov. *The Lancet Infectious Diseases*. 2014; 14(1): 6-7.

[4] Kermack WO, McKendrick AG. A contribution to the mathematical theory of epidemics. *Proceedings of the Royal Society of London Series A, Containing Papers of a Mathematical and Physical Character*. 1927; 115(772): 700-721.

[5] Assiri A, Al-Tawfiq JA, Al-Rabeeah AA, Al-Rabiah FA, Al-Hajjar S, Al-Barrak A, et al. Epidemiological, demographic, and clinical characteristics of 47 cases of Middle East respiratory syndrome coronavirus disease from Saudi Arabia: A descriptive study. *The Lancet Infectious Diseases*. 2013; 13(9): 752-761.

[6] Zumla A, Hui DS, Perlman S. Middle East respiratory syndrome. *The Lancet*. 2015; 386(9997): 995-1007.

[7] Anjam YN, Yavuz M, Rahman Mu, Batool A. Analysis of a fractional pollution model in a system of three interconnecting lakes. *AIMS Biophysics*. 2023; 10(2): 220-240.

[8] Haidong Q, Rahman Mu, Arfan M, Salimi M, Salahshour S, Ahmadian A. Fractal-fractional dynamical system of typhoid disease including protection from infection. *Engineering with Computers*. 2021; 39: 1553-1562. Available from: https://doi.org/10.1007/s00366-021-01536-y.

[9] Zhang L, Rahman Mu, Haidong Q, Arfan M. Fractal-fractional anthroponotic cutaneous leishmania model study in sense of Caputo derivative. *Alexandria Engineering Journal*. 2022; 61(6): 4423-4433.

[10] Li B, Zhang T, Zhang C. Investigation of financial bubble mathematical model under fractal-fractional Caputo derivative. *Fractals*. 2023; 31(05): 1-13.

[11] Zhu X, Xia P, He Q, Ni Z, Ni L. Coke price prediction approach based on dense Gru and opposition-based learning salp swarm algorithm. *International Journal of Bio-Inspired Computation*. 2023; 21(2): 106-121.

[12] Joshi H, Yavuz M, Özdemir N. Analysis of novel fractional order plastic waste model and its effects on air pollution with treatment mechanism. *Journal of Applied Analysis & Computation*. 2024; 14(6): 3078-3098.

[13] Avcı İ. Spectral collocation with generalized Laguerre operational matrix for numerical solutions of fractional electrical circuit models. *Mathematical Modelling and Numerical Simulation with Applications*. 2024; 4(1): 110-132.

[14] Yapışkan D, Eroğlu BBİ. Fractional-order brucellosis transmission model between interspecies with a saturated incidence rate. *Bulletin of Biomathematics*. 2024; 2(1): 114-132.

[15] Kar N, Özalp N. A fractional mathematical model approach on glioblastoma growth: Tumor visibility timing and patient survival. *Mathematical Modelling and Numerical Simulation with Applications*. 2024; 4(1): 66-85.

[16] Bhatter S, Kumawat S, Bhatia B, Purohit SD. Analysis of Covid-19 epidemic with intervention impacts by a fractional operator. *An International Journal of Optimization and Control: Theories & Applications (Ijocta)*. 2024; 14(3): 261-275.

[17] Raeisi E, Yavuz M, Khosravifarsani M, Fadaei Y. Mathematical modeling of interactions between colon cancer and immune system with a deep learning algorithm. *The European Physical Journal Plus*. 2024; 139(4): 345.

[18] Naik PA, Yavuz M, Qureshi S, Owolabi KM, Soomro A, Ganie AH. Memory impacts in hepatitis C: A global analysis of a fractional-order model with an effective treatment. *Computer Methods and Programs in Biomedicine*. 2024; 254: 108306.

[19] Zhu X, Xia P, He Q, Ni Z, Ni L. Ensemble classifier design based on perturbation binary salp swarm algorithm for classification. *Computer Modeling in Engineering & Sciences*. 2023; 135(1): 653-671.

[20] Coulibaly BD, Ghizlane C, El Khomssi M. An approach to stochastic differential equations for long-term forecasting in the presence of α-stable noise: An application to gold prices. *Mathematical Modelling and Numerical Simulation with Applications*. 2024; 4(2): 165-192.

[21] Alderremy AA, Gómez-Aguilar JF, Aly S, Saad KM. A fuzzy fractional model of coronavirus (Covid-19) and its study with Legendre spectral method. *Results in Physics*. 2021; 21: 103773.

[22] Pandey P, Chu YM, Gómez-Aguilar JF, Jahanshahi H, Aly AA. A novel fractional mathematical model of Covid-19 epidemic considering quarantine and latent time. *Results in Physics*. 2021; 26: 104286.

[23] Khan AA, Amin R, Ullah S, Sumelka W, Altanji M. Numerical simulation of a Caputo fractional epidemic model for the novel coronavirus with the impact of environmental transmission. *Alexandria Engineering Journal*. 2022; 61(7): 5083-5095.
[24] Kumar S, Ahmadian A, Kumar R, Kumar D, Singh J, Baleanu D, et al. An efficient numerical method for fractional SIR epidemic model of infectious disease by using Bernstein wavelets. *Mathematics*. 2020; 8(4): 558.
[25] Abdo MS, Shah K, Wahash HA, Panchal SK. On a comprehensive model of the novel coronavirus (Covid-19) under Mittag-Leffler derivative. *Chaos, Solitons & Fractals*. 2020; 135: 109867.
[26] de Carvalho JPM, Moreira-Pinto B. A fractional-order model for Covid-19 dynamics with reinfection and the importance of quarantine. *Chaos, Solitons & Fractals*. 2021; 151: 111275.
[27] Alrabaiah H, Rahman MU, Mahariq I, Bushnaq S, Arfan M. Fractional order analysis of HBV and HCV co-infection under ABC derivative. *Fractals*. 2022; 30(01): 2240036.
[28] de Carvalho JPM, Rodrigues AA. Strange attractors in a dynamical system inspired by a seasonally forced SIR model. *Physica D: Nonlinear Phenomena*. 2022; 434: 133268.
[29] Li B, Zhang Y, Li X, Eskandari Z, He Q. Bifurcation analysis and complex dynamics of a Kopel triopoly model. *Journal of Computational and Applied Mathematics*. 2023; 426: 115089.
[30] Maurício de Carvalho JP, Rodrigues AA. SIR model with vaccination: Bifurcation analysis. *Qualitative Theory of Dynamical Systems*. 2023; 22(3): 105.
[31] Fatima B, Yavuz M, Rahman MU, Al-Duais FS. Modeling the epidemic trend of Middle Eastern respiratory syndrome coronavirus with optimal control. *Mathematical Biosciences and Engineering*. 2023; 20(7): 11847-11874.
[32] He Q, Xia P, Hu C, Li B. Public information, actual intervention and inflation expectations. *Transformations in Business & Economics*. 2022; 21(2C): 644.
[33] Fatima B, Yavuz M, Rahman Mu, Althobaiti A, Althobaiti S. Predictive modeling and control strategies for the transmission of Middle East respiratory syndrome coronavirus. *Mathematical and Computational Applications*. 2023; 28(5): 98.
[34] Webb GF. Population models structured by age, size, and spatial position. In: *Structured Population Models in Biology and Epidemiology*. Berlin, Heidelberg: Springer; 2008. p.1-49.
[35] Inaba H. Mathematical analysis of an age-structured SIR epidemic model with vertical transmission. *Discrete & Continuous Dynamical Systems-B*. 2006; 6(1): 69.
[36] Van den Driessche P, Watmough J. Reproduction numbers and sub-threshold endemic equilibria for compartmental models of disease transmission. *Mathematical Biosciences*. 2002; 180(1-2): 29-48.
[37] Lashari AA, Hattaf K, Zaman G, Li XZ. Backward bifurcation and optimal control of a vector borne disease. *Applied Mathematics & Information Sciences*. 2013; 7(1): 301-309.
[38] Gumel AB. Causes of backward bifurcations in some epidemiological models. *Journal of Mathematical Analysis and Applications*. 2012; 395(1): 355-365.
[39] Fatima B, Zaman G, Alqudah MA, Abdeljawad T. Modeling the pandemic trend of 2019 Coronavirus with optimal control analysis. *Results in Physics*. 2021; 20: 103660.
[40] Mahardika R, Widowati, Sumanto Y. Routh-hurwitz criterion and bifurcation method for stability analysis of tuberculosis transmission model. *Journal of Physics: Conference Series*. 2019; 1217(1): 012056. Available from: https://dx.doi.org/10.1088/1742-6596/1217/1/012056.
[41] LaSalle JP. Stability of nonautonomous system. *Nonlinear Analysis*. 1976; 61(1): 83-90.
[42] Fatima B, Alqudah MA, Zaman G, Jarad F, Abdeljawad T. Modeling the transmission dynamics of Middle Eastern respiratory syndrome coronavirus with the impact of media coverage. *Results in Physics*. 2021; 24: 104053.